ISSN 1330-3651 (Print), ISSN 1848-6339 (Online)
https://doi.org/doi.org/10.17559/TV-20250205002338
Original scientific paper

Research on Heat Transfer Performance Prediction of Heat Exchanger Using Improved Particle Swarm Optimization Algorithm

Shuicai QIU*, Lingyan ZHANG

Abstract: With the increase of running time, the heat exchanger will appear dirt and even blocked, affecting the performance of the equipment. In this paper, an adaptive particle cognitive domain method is proposed. In the particle position updating method, the particle moves to the current best position with the calculated best position as the center, the cognitive direction of the particle is determined as the direction, and the linear inertial descending weight is used to realize the particle optimization. Using three different particle swarm optimization algorithms, namely fixed weight particle swarm optimization, linear descending weight particle swarm optimization and step mass particle swarm optimization, the heat transfer performance prediction algorithm of heat exchanger is designed according to the basic calculation principle of heat transfer performance. Based on the imported data of the cold and hot side, the heat exchange performance of the heat exchanger is theoretically calculated by using the calculation software, and compared with the heat exchange performance data calculated according to the field measured data, the operation state of the heat exchanger can be qualitatively analyzed, and the theoretical basis for the intervention and maintenance of the heat exchanger can be provided.

Keywords: cognitive domain, heat exchanger; linear descending weight particle swarm; particle swarm optimization; performance prediction; stepped swarm particle swarm optimization

1 INTRODUCTION

Heat exchangers are key equipment in the process of energy utilization, and have important applications in the fields of nuclear power, solar high-temperature lava thermal power generation and heating [1, 2]. For example, all the equipment on the nuclear island of a nuclear power plant must be cooled by the equipment cooling water system, and heat exchangers are used for heat exchange in important systems such as the equipment cooling water system on the nuclear island, the cooling and treatment system of the refueling chamber of the nuclear island reactor and the spent fuel pool, and the auxiliary feed water pump system on the nuclear island [3], in the solar thermal power generation system with high temperature molten salt as the medium. Therefore, the reliability and heat transfer capacity of the heat exchanger are closely related to the energy utilization efficiency.

During the long-term use of the heat exchanger, different degrees of scaling will occur due to the influence of its own structure, water quality and flow rate [4]. When the heat exchange medium contains large particles or fiber material, it is easy to block the channel between the plates, resulting in increased thermal resistance, and the heat transfer capacity of the heat exchanger is reduced, affecting the heat exchange efficiency. At the same time, the flow resistance of the working medium in the heat exchange tube will increase, which will accelerate the corrosion and damage of the equipment [5]. At present, the research on heat exchanger fouling mainly focuses on the chemical cleaning technology of fouling [6] and the prediction of fouling thermal resistance. X-ray fluorescence spectroscopy was used to analyze the composition of insoluble substances in the scale of plate heat exchanger in a nuclear power plant [7], and chemical scale dissolution research was carried out on the scale composition by hydrochloric acid and citric acid, and the results showed that hydrochloric acid and citric acid had a better ability to dissolve scale. The fouling thermal resistance prediction algorithm can determine the abnormal state of equipment according to the changing law of temperature, flow and other parameters, and then carry out predictive maintenance. At present, fouling prediction algorithms are mainly divided into two kinds: the prediction algorithm based on fouling formation mechanism and the prediction algorithm based on real-time data. A heat exchange pipe fouling thermal resistance prediction model based on generalized regression neural network was established [8], which is suitable for the prediction of fouling thermal resistance in most water quality environments. Three BP neural network prediction models were established based on the pH value of cooling water [9], and the results showed that the prediction model based on principal component analysis was more accurate. The LSTM model for prediction of fouling thermal resistance was established based on pipeline flow, population temperature and pressure [10], and compared with SVM, MLP and GRU models, indicating that the LSTM model has high accuracy. By testing and measuring the particle fouling data of plate heat exchanger [11], the criterion equation that the Nusselt number of particle fouling growth varies with Reynolds number and Prandtl number is theoretically deduced. Computational fluid dynamics was used to numerically simulate fluid flow and heat transfer in heat exchangers at different speeds [12].

At present, the researches on scaling behavior of heat exchangers mainly focus on scaling growth and heat transfer mechanism, but there are few reports on heat transfer performance prediction. In addition to the influence of dirt, the operating performance of the heat exchanger also changes with the change of the system flow rate, heat load and fluid temperature, resulting in the fact that operating characteristics of the heat exchanger generally cannot meet the performance requirements of the design condition, and the state of fluctuation is difficult to judge whether the performance of the heat exchanger meets the design requirements through the field operation data. In this paper, an adaptive updating method is designed to redistribute the best position of particle motion in the particle swarm updating equation so as to improve the performance of the particle swarm optimization algorithm. The algorithm uses the feature weight filtering method to eliminate some redundant features, and effectively reduces the search scale of the subsequent improved particle swarm optimization algorithm. Two improvement strategies, adaptive weight and T-distribution perturbation, balance the global exploration and local development ability of PSO, improve the diversity of PSO, and ensure that the feature selection of Wrapper algorithm is not easily trapped in the local optimal, so as to improve the feature selection performance of the algorithm. The heat transfer performance prediction algorithm is designed and the software is written according to the basic principle of heat transfer performance calculation. The heat transfer performance of the heat exchanger in the exchanger unit is cold, and the heat transfer performance of the heat exchanger is calculated theoretically according to the parameters of the No. 1 heat exchange and hot side transport of a power station. Thus, the qualitative analysis of the running state of the heat exchanger is realized.

2 RELATED WORK

At present, many scientists have analyzed and studied heat exchange conditions in the direct contact heat exchanger. Therefore, it is necessary to conduct a detailed analysis of the heat transfer effect of the direct contact heat exchanger to provide support for subsequent analysis, and only by fully combining the experimental data with the prediction model can the heat transfer capacity be accurately predicted. Therefore, the selection of prediction model has become an important part of the prediction of heat transfer effect.

Scholars have studied many kinds of prediction models, and there are many kinds of commonly used models. Support vector machine has many advantages (such as strong computational adaptability) and good application prospects in prediction, classification, pattern recognition and regression [13]. For example, it is reported that support vector machine model [14] has good predictive ability to some extent; it is proposed to predict future seasonal electricity consumption [15]. Then it is found that support vector machine has high accuracy [16]. Therefore, it is necessary to develop extended support vector machines to improve the calculation effect and accuracy [17]. It is found that the prediction of liquid viscosity by LSSVM is close to the true value [18]. A new method is proposed for data that cannot be accurately measured [19]. The LSSVM model is applied to the monthly runoff prediction [20]. The introduction of upstream flow data conditions in the model can improve the accuracy of the model. Although the predictive power of LSSVM is accurate, in order to obtain better predictive results, the data needs to be processed and combined with LSSVM to obtain more accurate predictive accuracy.

In order to better process the information in the data, that is suitable for data with high volatility and instability [21], a new method combining EMD (Empirical Mode Decomposition) and RBF (Radial basis function network) neural network [22] is proposed for time series decomposition and decomposition data processing. By comparing the experimental data, EMD method is used to obtain IMF components and residuals, which can better analyze and interpret the data and improve the prediction accuracy. The prediction method should also determine the specific operational data, find a more suitable prediction model, and improve the prediction accuracy [23]. The signal is decomposed to different degrees, and then detailed analysis is carried out to determine which model to use. In this way, the experimental error can be reduced, the experimental data can be closer, and the prediction accuracy of the model can be improved [24].

The heat transfer is related to the economic benefits of the enterprise. Therefore, it is very important to test or predict its heat transfer and flow resistance performance. In practical engineering applications, the selection of plate heat exchanger usually needs to consider the heat transfer coefficient and pressure drop two factors. The heat transfer coefficient directly affects the heat exchange area of the plate heat exchanger. Under the same heat transfer, the higher the heat transfer coefficient, the smaller the heat exchange area, and the reduction of the heat exchange area will reduce the equipment cost, reduce the maintenance workload and operating costs. However, the higher the heat transfer coefficient, the plate heat exchanger will also produce a large pressure drop while carrying out efficient heat transfer. Therefore, in the design and application of plate heat exchangers, it is impossible to achieve ideal operation effect by simply emphasizing the heat transfer coefficient or pressure drop [25]. There are many factors that affect the performance of plate heat exchanger, such as the heat exchange area, plate thickness, ripple depth, ripple pitch, ripple angle and the length-width ratio of plate. For plate heat exchangers with specific conditions, their heat transfer coefficient, pressure drop and correlation between heat transfer and flow resistance criteria are generally obtained by experimental methods [26]. In order to improve the overall performance of particle swarm optimization (PSO), many improved algorithms have appeared in recent years, and one of the important research methods is to improve the performance by improving the updating equation of particles. A fitness distance ratio particle swarm optimization algorithm is presented in reference [27]. Particles not only learn from the current best particle and the best position by far, but also learn from the better particles around them. Literature [28] designed a particle swarm optimization algorithm with understanding to add one dimension to the original particle swarm search space to determine the current search direction. In this way, within a certain radius, the particle can find better information about the current surrounding, which is used for particle renewal. This method is especially effective when the best information of the current generation is difficult to obtain for a certain particle. The literature [29,30] updates the particle swarm velocity and position according to the worst information of the organism as far as possible away from the current worst position and the worst position of the particle so far.

3 DESIGN OF HEAT EXCHANGER HEAT TRANSFER PERFORMANCE PREDICTION ALGORITHM

3.1 Heat Transfer Performance Evaluation

Basic principle of heat exchanger:

$$Q = hA\Delta t \tag{1}$$

where Q is the heat transfer, h is the heat transfer coefficient, A is the heat transfer area, and t is the heat transfer temperature difference °C.

The total heat transfer coefficient $UA = hA$ was defined, and the total heat transfer efficiency of the heat exchanger was characterized by UA (Unmanned Aircraft).

For heat exchangers used in specific occasions, the UA value under design conditions should reach a certain value to ensure that the system heat load can be taken away by running a single cooling pump and a single heat exchanger. However, the UA value reflects the heat transfer characteristics under specific working conditions, which changes with the system flow rate, heat load and fluid temperature. Therefore, the UA value under normal operating conditions cannot reach this fixed value, and it is impossible to judge whether the performance of the heat exchanger meets the design requirements through the field operation measured data.

When the UA value calculated according to the actual test data is less than 90% of the theoretical UA value, it indicates that the scale of the heat exchanger has exceeded the design amount and needs to be maintained or replaced. Through the cycle calculation, the actual test UA value (including design dirt) and the theoretical calculation UA value (including design dirt) are constantly compared, the end of the cycle calculation conditions is set, and the UA (including design dirt) value is finally checked.

The logic of the heat exchanger heat transfer performance prediction and evaluation algorithm is shown in Fig. 1.

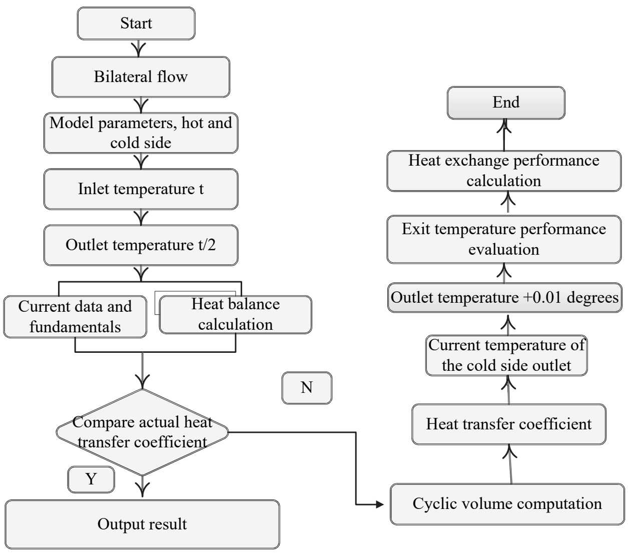

Figure 1 Heat exchanger heat transfer performance prediction and evaluation algorithm logic

The specific steps of prediction and evaluation are as follows: (1) The design margin of UA value of the heat exchanger under the design working condition is more than 10%, and the dirt coefficient is determined through the conversion of the margin. (2) Assuming that the flow rate on both sides of the heat exchanger and the inlet temperature are known, the outlet temperature of the cold side is set, and the heat transfer coefficient, heat load and logarithmic average temperature difference under the condition containing dirt are calculated through the heat balance. The actual heat transfer coefficient can be calculated. (3) Compare the actual test UA value with the theoretical calculation UA value, if not equal, continue to modify the cold side outlet temperature until the two are equal, indicating that the scale situation of the heat exchanger has reached the design critical point, at which time the UA value in the state containing dirt can be calculated.

3.2 Improved Method of Particle Swarm Optimization

Based on different particle cognition domains, the updating method of particle swarm optimization is improved.

The cognitive domain of this particle is defined by taking the best position of the particle calculated so far as the center, and the radius determined according to the current fitness of different particles is a certain region bounded by it. The boundary of this domain is called the maximum cognitive domain. The maximum cognitive domain of the i-th individual is expressed as follows:

$$MCD_i(t) = \max \frac{\max fit(t) - \min fit(t)}{fit(t)} \tag{2}$$

where, max is the best fitness value obtained by the particle so far and the current fitness value of the particle respectively; w is the inertia weight of the particle.

In the process of particle swarm iteration, the algorithm needs to increase the particle change step in the early stage of iteration, so as to locate the region is located earlier. In the later stage of the algorithm iteration, it is necessary to reduce the particle change step to make the particle search in this region fine. Based on the above ideas, this paper proposes an adaptive inertial weight strategy to balance the global exploration and local development ability of the algorithm. Calculation of w:

$$w = \frac{4}{5} \times e^{-\frac{t}{t_{\max}}} \tag{3}$$

where, t represents the number of iterations and $t_{\max}$ represents the maximum number of iterations. w at the early stage of iteration, the maximum value is taken as much as possible, so that the algorithm step size changes rapidly, which is convenient for global search. With the progress of iteration, the weight is reduced and the local search is emphasized. This strategy effectively balances the ability of global exploration and local development.

The flow of the algorithm is shown in Fig. 2.

At the beginning of the iteration, the individual diversity of the particle population decreased rapidly, resulting in a low population diversity in the later iteration. When the group optimal value of a particle swarm is far from the global optimal value, the particle is easy to evolve and learn in the wrong direction, and it is easy to fall into the local optimal value. The perturbation strategy based on T-distribution can increase the diversity of particle population and jump out of local optimal in time during algorithm iteration. That is, if after several successive iterations, the optimal fitness value of the current particle basically does not change or no longer changes, it is considered that the algorithm is trapped in the local optimal, and at this time, perturbation is added to make the particle shake, making it jump out of the local optimal, which also increases the population diversity. The policy is as follows:

$$X_i^t = X_i + X_i * h(t) \tag{4}$$

where, X_i^t represents the particle position after the disturbance; $h(t)$ represents the value of the T-distribution with the current iteration number t as the degree of freedom. By changing the functional form of $h(t)$ growing with t (linear, non-linear, logarithmic, exponential, etc.), parameters are introduced to control the growth rate or upper and lower limits, ensuring that the degree of freedom is always valid (≥1).

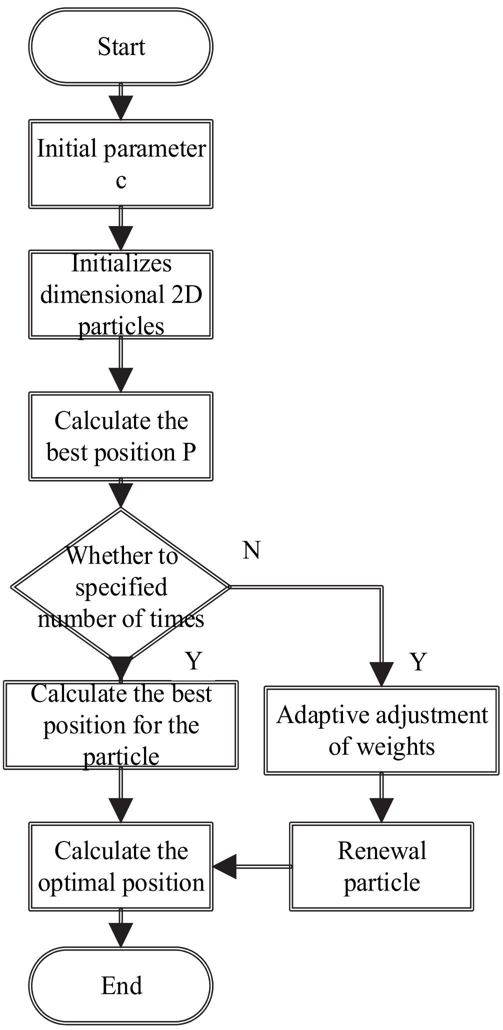

Figure 2 Flowchart of adaptive inertial weight strategy algorithm

The feature selection of data sets can be transformed into a multi-objective optimization problem. The optimization goal is to minimize the number of feature selections and maximize the classification accuracy of the classifier. Based on the above two optimization objectives, this paper defines the fitness function as:

$$fit = \alpha \times error_{rate} + \beta \frac{RF}{D} \tag{5}$$

where, error rate represents the error rate of the specified classification algorithm, D represents the total number of features of the samples in the data set, RF represents the size of the feature subset finally selected by the feature selection algorithm, α, β respectively correspond to the importance of the error rate of the classification algorithm and the size of the feature subset in the fitness. Detailed steps of the algorithm are shown in Tab. 1 below:

Table 1 Improved particle swarm optimization algorithm

Input: baseline data set.
Output: The optimal feature subset and the accuracy of the classificational gorithm.
Step 1 Input the baseline data set and divideit into the training set and the test set in a ratio of 7:3.
Step 2 Use the RELIEF-F algorithm to calculate the weight of each feature
The weights sort the features.
Step 3 Filter the ordered feature set according to the set stop value.
Step 4 Initialize the parameters of the particle swarm optimization algorithm, initialize the initial particle position, and map the particle position to the feature set.
Step 5 Calculate the particle fitness value.
Step 6 Comparethe fitness values of each particle and update the global and local optimal solutions.
Step 7 Update particle positions using the adaptive inertial weight strategy.
Step 8 Run the T-distribution policy.
Step 9 If the number of iterations has not reached the upper limit, go to Step 5.
Step 10 Output the optimal feature subset and classification accuracy.

4 APPLICATION ANALYSIS OF HEAT TRANSFER PERFORMANCE PREDICTION ALGORITHM FOR HEAT EXCHANGERS

Based on the calculation of heat transfer performance, 18 operating points were selected from the lowest temperature to the highest temperature to calculate the measured data based on the annual operating sea water temperature change of the plate heat exchanger site, 18 of which were designed conditions. In addition, the comparative analysis also considered the pipeline, measuring points, equipment accuracy and other issues: (1) the hot side flow under the working condition 1-10 is the total flow, but there is a bypass in the pipeline, the actual flow into the heat exchanger will be reduced. (2) The temperature measurement point of the cold side population is far away from the population section of the heat exchanger. Compared with the previous thermal test data, this temperature value is higher than the actual temperature value of the heat exchanger. Therefore, the field data are processed and corrected in the subsequent calculation. The comparison between the software modified *UA* value of the heat exchanger and the measured *UA* value is shown in Tab. 2. It should be noted that the *UA* limit is 10% lower than the software-corrected *UA* value in Tab. 2. The deviation of *UA* value in Tab. 2 is = (measured *UA* value − software corrected *UA* value)/measured *UA* value. If this value is lower than −10%, it indicates that the measured *UA* value is less than 90% of the theoretical calculated *UA* value, and the heat exchange equipment needs maintenance intervention.

Table 2 Comparison between the modified particles warm optimization and the measured value of heat exchanger

Working condition	Inlet temperature of the hot side / °C	Temperature at the hot side outlet / °C	Hot side corrected volume flow	Cold side inlet modified temperature /°C	Cold side outlet temperature /°C	Cold side volume flow	Actual *UA* value	Algorithm modification *UA*	*UA* value deviation
1	7.s7	24.56	1 001.07	26.36	19.60	2 478.29	3 602.76	4 113.90	−12.42
2	8.44	25.59	989.40	27.24	20.50	2 481.67	3 695.14	4 088.70	−9.63
3	9.64	26.68	981.62	28.38	21.71	2 484.17	3 611.42	4 106.70	−12.06
4	10.41	27.57	973.91	29.08	22.44	2 478.55	3 758.23	4 113.00	−8.63
5	13.83	29.93	006.56	30.90	24.47	2 483.86	4 571.44	4 234.50	7.96
6	14.94	31.26	997.15	32.17	25.72	2 483.37	4 640.29	4 253.40	9.10
7	14.60	27.14	426.43	28.93	22.40	2 482.94	4 993.34	4 784.40	4.37
8	16.86	28.52	416.43	30.34	23.69	2 446.55	4 964.07	4 794.30	3.54
9	17.82	29.41	393.32	31.05	24.54	2 446.65	5 116.04	4 793.40	6.73
10	18.78	30.30	376.71	31.87	25.47	2 442.49	5 118.26	4 797.90	6.68
11	23.34	28.90	2 928.69	32.17	25.71	2 478.26	6 631.27	6 053.40	9.55
12	24.49	30.04	2 935.77	33.28	26.80	2 478.85	6 749.82	6 098.40	10.68
13	24.32	30.85	2 936.40	34.06	27.60	2 475.22	6 802.51	6 124.50	11.07
14	26.29	32.22	2 960.80	35.73	28.72	2 472.22	6 810.44	6 183.00	10.15
15	27.34	33.25	2 960.45	36.92	29.86	2 444.20	6 514.00	6 201.00	5.05
16	28.36	34.13	2 882.12	37.40	30.82	2 488.57	6 653.28	6 229.80	6.80
17	29.66	35.39	2 880.77	38.71	32.07	2 489.34	6 599.73	6 279.30	5.10
18	33.89	44.20	2 680.07	49.07	37.78	2 434.55	7 199.51	7 156.00	11.79

Measured *UA* value − algorithm modified *UA* value)/ measured *UA* value, if this value is lower than −10%, it indicates that the measured *UA* value is less than 90% of the theoretical calculated *UA* value, and the heat exchange equipment needs maintenance intervention.

In view of the inevitable errors of instruments and other instruments in the actual measurement process, it is acceptable that the deviation between the software's calculated *UA* value and the field measured *UA* value is less than 10% according to the acceptance requirements determined in "Evaluation of Heat Transfer Performance of a Plate Heat Exchanger". Therefore, in order to avoid the influence of data error, 10% of the *UA* value calculated by the software is taken as the *UA* limit of the corresponding working condition. If the field measured *UA* value is lower than the *UA* limit, it indicates that the plate fouling coefficient is too large, and maintenance intervention is needed. The comparison between the software calculated *UA* value and the measured *UA* value of the plate heat exchanger under different working conditions is shown in Fig. 3.

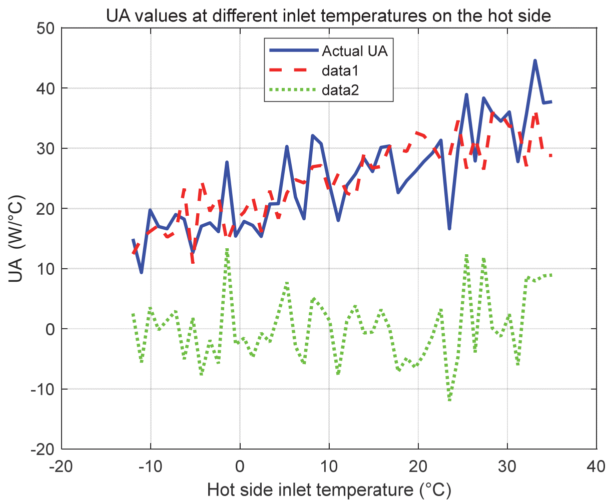

Figure 3 Comparison between the software modified *UA* value of heat exchanger and the measured *UA* value under different working conditions

It can be seen from the data in Tab. 2 and Fig. 3 that the measured *UA* value of working conditions 1 to 4 is lower than that calculated by the software. In fact, the temperature of seawater side in working condition 1-4 is low and there is a side flow. Even if the cold side corresponds to the highest temperature in the design working condition, the heat exchange margin of the heat exchanger is still large. Therefore, the deviation of *UA* value in working condition 1-4 is mainly caused by a certain deviation after correction of the measured data.

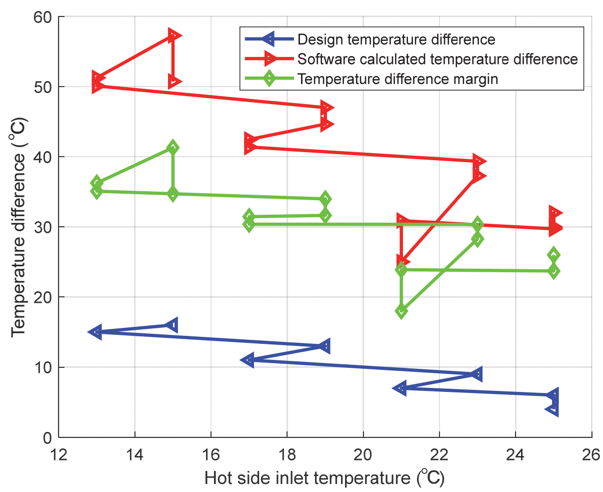

Figure 4 Calculation results of temperature difference and margin of heat exchanger when the cold side is the design working parameter and the hot side has side flow

The working conditions 1-10 with side-flow on the hot side are further analyzed and calculated. The measured population temperature and flow value of seawater under working conditions 1-10 were adopted on the hot side, while the temperature and flow value under design working conditions were adopted on the cold side. The results of calculation and analysis are shown in Fig. 4. It can be seen from Fig. 4 that under the design working parameters of the cold side, the heat exchanger still has a large temperature difference margin, indicating that compared with the design working conditions, the heat exchanger still has a large heat exchange margin. When dirt increases in the operation of the heat exchanger and the heat transfer performance of the equipment decreases, the performance of the heat exchanger can be adjusted by increasing the seawater flow rate to meet the design requirements.

On this basis, the heat exchanger performance under full flow on the hot side was calculated and analyzed, that is, the measured sea water temperature and total sea water flow corresponding to working conditions 1-10 were used on the hot side, and the temperature and flow values under design working conditions were used on the cold side. The calculation results are shown in Fig. 5. As shown in Fig. 5, when the side-flow is not turned on on the hot side, the temperature difference margin corresponding to working conditions 1-10 exceeds 100%.

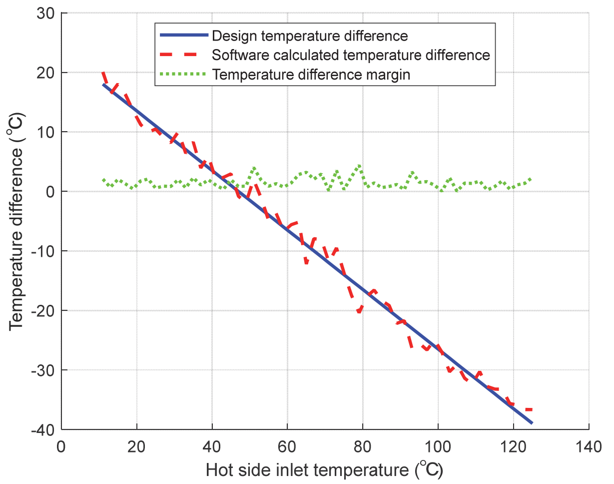

Figure 5 Calculation results of temperature difference and margin of heat exchanger when the cold side is the design working parameter and there is no side flow on the hot side

It can be seen that the *UA* value of the heat exchanger can effectively find out the abnormal state of the equipment, and judge the heat transfer performance of the equipment, and realize predictive maintenance.

5 SIMULATION VERIFICATION

The experimental data was modeled using a combination of the Empirical Mode Decomposition (EMD) method and a Support Vector Machine (SVM). EMD was employed to standardize the data decomposition process, followed by an analysis of the pulse sequence to isolate and process the signal related to the volume heat transfer coefficient. Fig. 6 illustrates the original volume heat transfer coefficient signal, denoted as H, which exhibits complex fluctuations and lacks a discernible pattern. Through EMD decomposition, the signal was divided into six Intrinsic Mode Functions (IMFs) and one residual component, with IMFs 1 to 6 ordered from highest to lowest frequency. The decomposed signals displayed enhanced stability and regularity compared to the original. These graphical representations clearly depict the time-varying nature of the mean volume heat transfer coefficient, characterized by irregularity, fluctuation, and nonlinearity. The findings underscore EMD's effectiveness in data processing and decomposition.

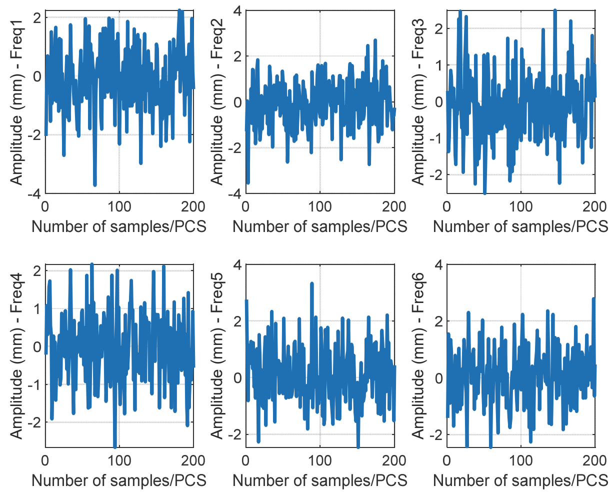

Figure 6 EMD decomposition results of the original volume heat transfer coefficient signal

This section integrates the Least Squares Support Vector Machine (LSSVM) with Empirical Mode Decomposition (EMD) to standardize the volume heat transfer coefficient data. Fig. 7 presents the results, where the *X*-axis spans data points from 345 to 450. The predicted volumetric heat transfer coefficient axis displays values ranging from 0 to 0.6, obtained using the combined model. The real volumetric heat transfer coefficient axis, reflecting experimental values, covers the range of 0 to 0.6. Observing Fig. 7, we notice minor prediction discrepancies within the ranges of 360-380 and 430-440, with more pronounced errors near the data point of 400. For most other data points, the predicted values closely align with the real values, indicating a satisfactory prediction performance. In summary, the comparison reveals that the predicted and real values exhibit minimal divergence and share a similar trend, attesting to a prediction effect on par with simulation outcomes. This validates the model's efficacy and confirms the feasibility of combining EMD with LSSVM.

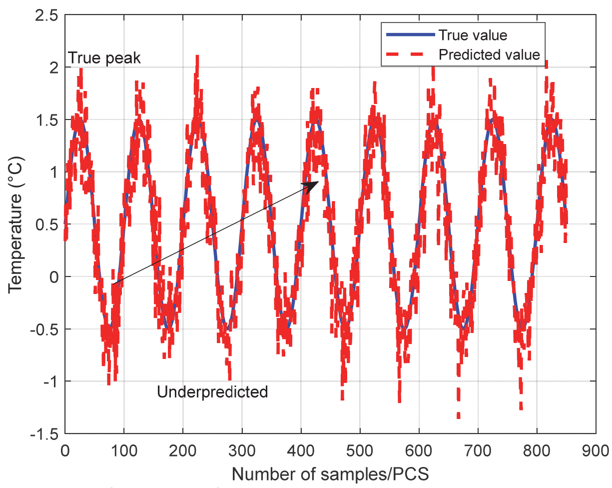

Figure 7 Comparison of the relationship between the real value and the predicted value of the volumetric heat transfer coefficient data

The performance of the heat exchanger was evaluated according to the improved particle swarm optimization algorithm established in the paper, and the results are shown in Tab. 3. Tab. 3 shows the comparison between the experimental and predicted values of the heat transfer coefficient K of the heat exchanger, the pressure drop on the hot and cold side, and the correlation formula of heat transfer criteria. The predicted results are close to the experimental ones. It can be seen from Tab. 3 that there is a large error in the prediction of sample point 12. The main reasons are as follows.

Table 3 Comparison of experimental and predicted values of heat exchanger

No.	Item	K	Ph	Pc	Ch	P
1	Experiment	5 015	51 .9	56.12	0. 15	0.729
2	Forecast	5 008	51 .6	56.24	0. 15	0.730
3	Error	0.139	0. 578	−0.213	0. 000	−0.041
4	Experiment	5 514	33. 0	31 .0	0. 230	0.699
5	Forecast	5 525	32. 5	31 .0	0. 228	0.699
6	Error	−0. 199	1 .515	0. 000	1 .087	0.071

(1) The sample database is not perfect enough, and the accuracy of some special prediction objects is bound to be reduced. With the enrichment and improvement of the experimental database in the future and the increase of the sample library capacity, the heat transfer and flow resistance performance of the same series of heat exchangers under the same operating conditions can be evaluated quickly and accurately.

(2) Due to the limitations of existing experimental data, many apparent indicators were selected. In order to improve the prediction accuracy, it is necessary to choose more sensitive and easier to quantify input parameters, such as the thermal conductivity of the plate material, the specific parameters of the plate ripple form. The calculated average error rate is 0.303, and the simulation accuracy is up to 99.696%. From the error, it can be seen that the predicted value of the particle swarm optimization model is close to the experimental value, indicating that the improved particle swarm optimization model has strong prediction ability and can fully achieve the accuracy of practical application.

In the process of continuous casting, the surface temperature at the end of the first section of the secondary cooling zone cannot be measured due to site conditions. In this case, it is necessary to use the known temperature at the end of the third section of the secondary cooling zone to identify the four accurate heat transfer coefficients of the secondary cooling zone, so as to obtain the accurate surface temperature at the end of the first section of the secondary cooling zone. According to the study on the relationship between the heat transfer coefficient of secondary cooling and the amount of water, the identification parameters a_1 and a_2 are less than a_3 and a_4 under the constraint conditions, and the heat transfer coefficients of the four stages in the secondary cooling zone of continuous casting are still set as $a_1 = 2.3$, $a_2 = 2.6$, $a_3 = 3.2$, $a_4 = 3.8$. In order to find the optimal solution of the secondary cooling heat transfer coefficient, the learning factors c_1, c_2 and inertia weight w in chaotic particle swarm are restricted. The optimizations work best when the sum of c_1, c_2 is less than 3. By using the asynchronous change strategy factor, the particles can learn more from the social optimal solution and less from the self-optimal solution, so that the particles have a fast convergence speed and keep the particle diversity. The limitations of inertia weight w and learning factors c_1 and c_2 are as follows:

$$\begin{aligned} c_1 &= c_{1i} - \frac{k}{w_{\max}} \\ c_2 &= c_{2i} - \frac{k}{w_{\max}} \end{aligned} \tag{6}$$

Fig. 8 shows the convergence process of the constrained improved particle swarm optimization algorithm.

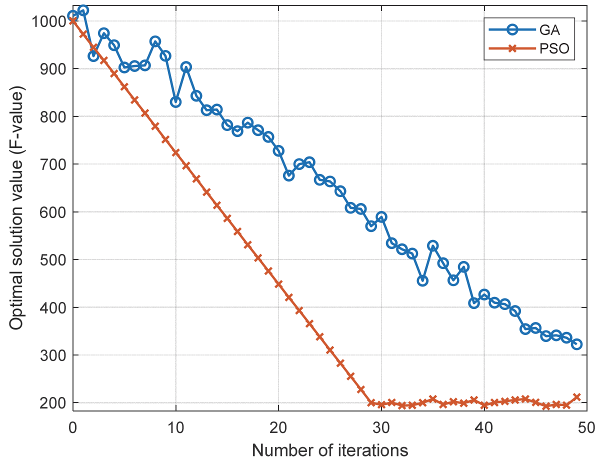

Figure 8 Convergence process of improved particle swarm optimization algorithm

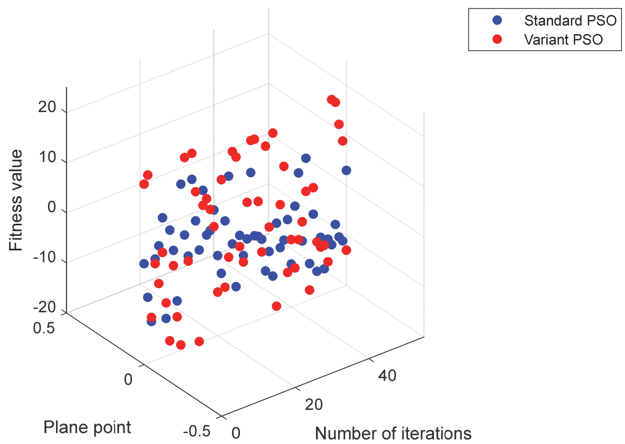

Figure 9 Average fitness curve of population

The performance of automata is evaluated by using improved particle swarm optimization algorithm and floating heat transfer curve of heat exchanger. As can be seen from Fig. 9, the particle swarm optimization algorithm has good convergence in the process of optimization. However, from the perspective of convergence speed, although the average fitness of the initial population of standard PSO is obviously better than that of improved PSO, the convergence speed still declines and almost stops in the later period, while the PSO with variable w can enter the local search quickly and has a good convergence speed. From the results of the optimal solution, as shown in Tab. 4, the particle swarm optimization algorithm combined with the characteristic quantity of the curve was used to obtain the solution of the performance parameters of each mechanism basically consistent with the set values. However, from the perspective of accuracy, the global optimal solution obtained by the PSO with variation and variable w was obviously superior to the standard PSO, and the PSO with variation was the closest to the set values and had better accuracy. It is feasible to apply this method to the state parameter evaluation of mechanism.

Table 4 Comparison of algorithm results

Set value	Standard PSO	Change to *w* PSO	Change *w*, change PSO
7.5	7.16	6.3022	6.5051
50%	59.05%	47.35%	50.05%
15.4	15.411	15.3986	15.4014

Heat transfer performance prediction and parameter sensitivity analysis. The improved particle swarm optimization algorithm established and optimized above was used to predict the heat transfer performance of the heat exchanger, and all 38 sample data were used for performance prediction. Fig. 10 shows the comparison between the predicted value of the network and the experimental value. It can be seen that the trends of the two are very consistent. The maximum and average relative errors of the network prediction are 14% and 3.86% respectively, that is, except for 2 samples, the network prediction performance of the other samples is very close to the experimental value.

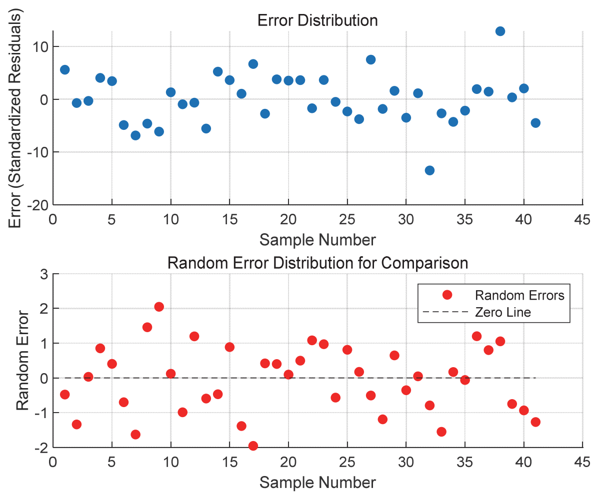

Figure 10 Comparison between heat transfer performance prediction and experimental data

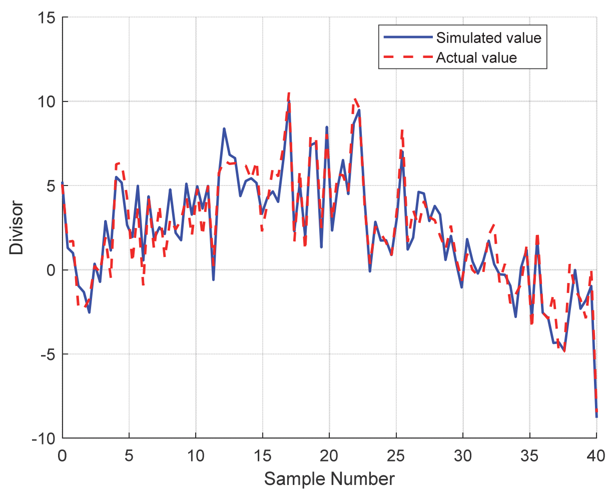

Figure 11 Comparison between flow resistance performance prediction and experimental data

Flow Performance Prediction and parametric sensitivity analysis. All 38 sample data were used to predict the flow resistance characteristics of heat exchangers. Fig. 11 shows the comparison between the predicted value of the network and the experimental value. It can be seen that the trends of the two are consistent. The average relative error of flow resistance network prediction is 6.8%, that is, except for 2 samples, the network prediction performance of the other samples is close to the experimental value.

The above analysis process shows that the improved particle swarm optimization algorithm can be applied to predict the flow heat transfer performance of heat exchanger, and the parameter sensitivity can be obtained by combining with the sensitivity analysis method. This can reduce the workload of experiment and simulation to a certain extent, and can be used to analyze the sensitivity of heat exchanger fin parameters, and provide directional guidance for heat exchanger optimization design. However, it should be noted that for the heat transfer and flow resistance performance of the heat exchanger, the network modeling, training, optimization and prediction should be carried out respectively to solve the contradiction between the two, and the flow resistance is often increased while improving the heat transfer performance.

Under different cold and hot side flows, the comparison between the experimental results of the cooler and the numerical simulation results is shown in Fig. 12, where the hot side flows are 560 kg/hr, 721 kg/hr, 974 kg/hr, respectively.

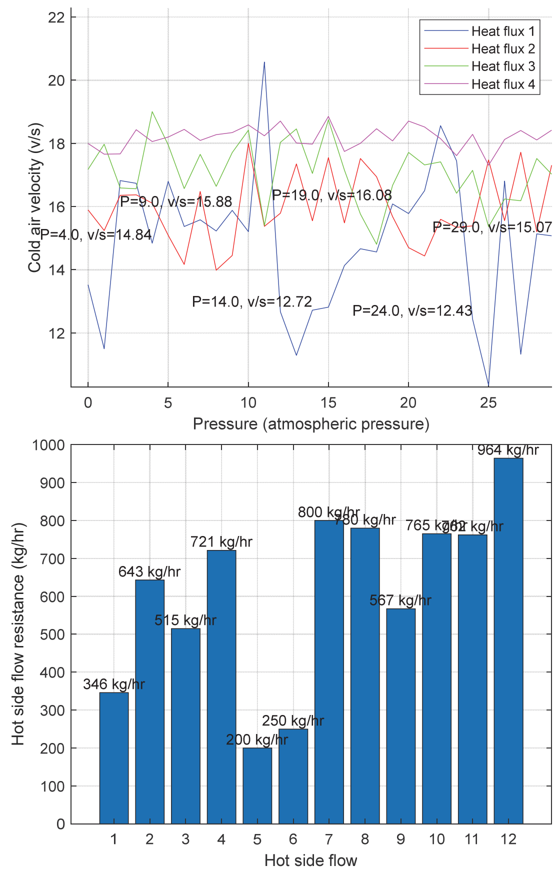

Figure 12 Comparison between experimental results and simulation results of thermal performance of cooler

As can be seen from Fig. 12, the simulation results of the thermal performance of the cooler are consistent with the trend of the experimental data. When the porous medium model is used for thermal performance simulation, the maximum deviation between the simulation results of heat transfer performance and the experimental data is nearly 30%, and the maximum flow resistance is about 15%.

6 CONCLUSION

The improved particle swarm optimization algorithm is used to establish the prediction model, and the structure of the improved particle swarm optimization algorithm is reasonably designed according to the analysis of the plate parameters and the flow channel form. The performance of plate heat exchangers with single beam ripple, sine wave cross section and qualitative temperature of 40 ℃ is predicted. The prediction results show that the prediction accuracy of this network is very high and can reach or even exceed the accuracy of practical engineering applications. The improved particle swarm optimization (PSO) to predict the heat transfer and flow resistance performance of heat exchangers is of great value to the development and selection calculation of heat exchangers. It is worth noting that in order to make a more accurate prediction of an object, the first thing is to ensure that the training samples must be accurate and the number of training samples should be sufficient. The theoretical calculation algorithm of heat transfer characteristics of heat exchanger and the algorithm software are compiled. By comparing the theoretical *UA* value calculated by software with the *UA* value calculated by field measured data, the operating characteristics of plate heat exchanger can be judged, abnormal state can be found effectively, and predictive maintenance can be achieved. In this paper, the traditional decomposition method is adopted in the process of time series decomposition. The subsequent work can be decomposed for the study of better data decomposition methods to improve the prediction accuracy of volumetric heat transfer coefficient.

Acknowledgment

The work was supported by Industry-education cooperation and Collaborative education project of the Ministry of Education (No: 230904973224504); and the First-class professional project of Changzhou University Huaide College (No: 1511010002).

7 REFERENCES

[1] Alqaed, S., Mustafa, J., & Sajadi, S. M. (2024). The effect of turbulator holes diameter on heat transfer optimization of a geothermal heat exchanger by using nanofluid. *Geothermics*, *119*, 2967-2986. https://doi.org /10.1016/j.geothermics.2024.102967

[2] Ouabouch, O., Laasri, I. A., & Kriraa, M. (2023). Investigation of novel turbulator with and without twisted configuration under turbulent forced convection of a CuO/water nanofluid flow inside a parabolic trough solar collector. *AIMS Materials Science*, *10*(1), 7-26. https://doi.org /10.3934/matersci.2023007

[3] Sun, K., Liu, D., & Ghoushchi, S. P. (2023). Heat transfer and pressure drop in a double pipe exchanger equipped with novel perforated magnetic turbulator (PMT): An experimental study. *Applied Thermal Engineering*, *235*, 1278-1295. https://doi.org/10.1016/j.applthermaleng.2023.121278

[4] Mohammad, Z., Seyfolah, S., & Nader, M. K. (2023). Recent progress on flat plate solar collectors equipped with nanofluid and turbulator: state of the art. *Environmental Science and Pollution Research*, *30*(51), 109921-109954. https://doi.org/10.1007/s11356-023-29815-9

[5] Ibrahim, M., Abidi, A., & Algehyne, E. A. (2022). Improvement of the energy and exergy efficiencies of the parabolic solar collector equipped with a twisted turbulator using SWCNT-Cu/water two-phase hybrid nanofluid. *Sustainable energy technologies and assessments*, *2022*(Feb.), 49-75. https://doi.org/10.1016/j.seta.2021.101705

[6] Baklouti, A., Dammak, K., & El Hami, A. (2022). Optimum reliable design of rolling element bearings using multi-objective optimization based on C-NSGA-II. *Reliability Engineering and System Safety*, *223*, 508-521. https://doi.org/10.1016/j.ress.2022.108508

[7] Feng, L. & Zhang, L. (2022). Enhanced prediction intervals of tunnel-induced settlement using the genetic algorithm and neural network. *Reliability Engineering & System Safety*, *223*, 108439-108454. https://doi.org/10.1016/j.ress.2022.108439

[8] Guan, Y., Wang, L., & Cui, H. (2023). Optimization Analysis of Thermodynamic Characteristics of Serrated Plate-Fin Heat Exchanger. *Sensors (14248220)*, *23*(8), 158-167. https://doi.org/10.3390/s23084158

[9] Alfwzan, W. F., Alomani, G. A., & Alessa, L. A. (2024). Sensitivity Analysis and Design Optimization of Nanofluid Heat Transfer in a Shell-and-Tube Heat Exchanger for Solar Thermal Energy Systems: A Statistical Approach. *Arabian Journal for Science and Engineering*, *49*(7), 9831-9847. https://doi.org/10.1007/s13369-023-08568-0

[10] Alyaseen, N. O. M., Mehrzad, S., & Saffarian, M. R. (2023). Design of the Multistream Plate-Fin Heat Exchanger in the Air Separation Units. *International Journal of Heat & Technology*, *41*(1), 120-133. https://doi.org/10.18280/ijht.410120

[11] Zhu, C. (2024). Research on the Heat Transfer Performance of Phase Change Heat Storage Heat Exchangers Based on Heat Transfer Optimization. *Energies*, *17*, 150-167. https://doi.org/10.3390/en17164150

[12] Fu, B., Guo, Z., & Yan, J. (2023). Research on the Heat Extraction Performance Optimization of Spiral Fin Coaxial Borehole Heat Exchanger Based on GA-BPNN-QLMPA. *Processes*, *11*(10), 2989-3002. https://doi.org/10.3390/pr11102989

[13] Jingde, Z., Jie, F., & Chang, D. U. (2021). Numerical simulation of the effect of fin length on melting process of phase change materials. *Journal of Donghua University (Natural Science Edition)*, *47*(4), 264-278. https://doi.org/10.19886/j.cnki.dhdz.2020.0264

[14] Ahirwar, B. K. & Kumar, A. (2024). Enhancing thermal performance: a sophisticated analysis of CuO-water nanofluids and twisted tape inserts in tubular heat exchangers-a numerical study. *Journal of Thermal Analysis and Calorimetry*, *149*(24), 15323-15337. https://doi.org/10.1007/s10973-024-13860-8

[15] Sai, J. P. & Rao, B. N. (2022). Non-dominated Sorting Genetic Algorithm II and Particle Swarm Optimization for design optimization of Shell and Tube Heat Exchanger. *International Communications in Heat and Mass Transfer: A Rapid Communications Journal*, *2022*(132), 132-156. https://doi.org/10.1016/j.icheatmasstransfer.2022.105896

[16] Simari, C., Lufrano, E., & Lemes, G. (2021). Electrochemical Performance and Alkaline Stability of Cross-linked Quaternized Polyepichlorohydrin/PvDF Blends for Anion-Exchange Membrane Fuel Cells. *The Journal of Physical Chemistry C*, *125*(10), 5494-5504. https://doi.org/10.1021/acs.jpcc.0c11346

[17] Cao, W., Wei, F., & Liu, F. (2022). Experimental study on flow and heat transfer performance of condensing gas-fired boiler. *Journal of Physics: Conference Series*, *2401*(1), 12015-12028. https://doi.org/10.1088/1742-6596/2401/1/012015
[18] Mccaughtry, T. & Kim, S. I. (2021). Multi-objective optimization tool of shell-and-tube heat exchangers using a modified teaching-learning-based optimization algorithm and a compact Bell-Delaware method. *Heat Transfer Engineering*, *2021*, 1-17. https://doi.org/10.1080/01457632.2021.1943836
[19] Yang, L., Xu, H., & Cola, F. (2021). Shell-and-Tube Latent Heat Thermal Energy Storage Design Methodology with Material Selection, Storage Performance Evaluation, and Cost Minimization. *Applied Sciences*, *11*, 4180-4193. https://doi.org/10.3390/APP11094180
[20] Gugulothu, R., & Sanke, N. (2022). Effect of helical baffles and water-based Al_2O_3, CuO, and SiO_2 nanoparticles in the enhancement of thermal performance for shell and tube heat exchanger. *Heat Transfer*, *51*, 3768-3793. https://doi.org/10.1002/htj.22474
[21] Makadia, J. & Sankhavara, C. D. (2021). Optimization of Shell and Tube Heat Exchanger Using Alpha Tuning Elephant Herding Optimization (EHO) Technique. *International Journal of Engineering Research in Africa*, *52*, 92-101. https://doi.org/10.4028/www.scientific.net/JERA.52.92
[22] Wu, X., Xu, J., & Hu, Y. (2021). Improved Heat Exchanger Network Synthesis without Stream Splits Based on Comprehensive Learning Particle Swarm Optimizer. *ACS omega*, *6*(44), 29459-29470. https://doi.org/10.1021/acsomega.1c03424
[23] Dou, Q., Pan, H., &Wang, J. H. (2024). Program synthesis algorithm based on context consistency heuristic. *International journal of machine learning and cybernetics, 15*(2), 559-571. https://doi.org/10.1109/TNNLS.2023.2227339
[24] Sharma, O., Sharma, A., & Kalia, A. (2024). MIGAN: GAN for facilitating malware image synthesis with improved malware classification on novel dataset. *Expert Systems with Application*, *241*(May), 122678.1-122678.22. https://doi.org/10.1016/j.eswa.2023.122678
[25] Kathirvel, I. & Ganesan, N. G. (2024). Computational Strategies to Enhance Cell-Free Protein Synthesis Efficiency. *Bio Med Informatics*, *4*(3), 110-124. https://doi.org/10.3390/biomedinformatics4030110
[26] Kim, D. W., Sin, G. Y., & Kim, K. (2024). Network Traffic Synthesis and Simulation Framework for Cybersecurity Exercise Systems. *Computers, Materials & Continua*, *2024*, *80*(3), 3637-3653. https://doi.org/10.32604/cmc.2024.054108
[27] Zhang, H., Ren, G., & Jia, P. N. (2024). Development of machine learning force field for thermal conductivity analysis in MoAlB: Insights into anisotropic heat transfer mechanisms. *Ceramics International*, *50*(8), 13740-13749. https://doi.org/10.1016/j.ceramint.2024.01.288
[28] Górecki, G., Cki, M., & Gutkowski, A. N. (2021). Experimental and Numerical Study of Heat Pipe Heat Exchanger with Individually Finned Heat Pipes. *Energies*, *14*. https://doi.org/10.3390/en14175317
[29] Jin, H., Wang, M., & Xiang, H. (2024). A PSO-RBF prediction method on flow corrosion of heat exchanger using the industrial operations data. *Process Safety and Environmental Protection*, *183*, 11-23. https://doi.org/10.1016/j.psep.2024.01.001
[30] Ahamad, S. & Verma, S. K. (2024). Experimental investigation on thermo-hydraulic performance of three fluid heat exchanger using passive technique for heat transfer enhancement. *Thermal science and engineering progress*, *53*, 102733-102754. https://doi.org/10.1016/j.tsep.2024.102733

Contact information:

Shuicai QIU
(Corresponding author)
Department of Mechanical and material engineering,
Changzhou University, Huaide College,
Jingjiang, 214500, China
E-mail: qiushuicai_czuh@163.com

Lingyan ZHANG
Department of Mechanical and material engineering,
Changzhou University, Huaide College,
Jingjiang, 214500, China